# Numerical Simulation of Rocket Engine Internal Flows

Project Representative
Kozo Fujii JAXA's Engineering Digital Innovation Center, Japan Aerospace Exploration Agency

Authors
Taro Shimizu JAXA's Engineering Digital Innovation Center, Japan Aerospace Exploration Agency
Nobuhiro Yamanishi JAXA's Engineering Digital Innovation Center, Japan Aerospace Exploration Agency
Chisachi Kato Institute of Industrial Science, The University of Tokyo
Nobuhide Kasagi Department of Mechanical Engineering, The University of Tokyo
Kaoru Iwamoto Department of Mechanical Engineering, Tokyo University of Science

This year, one of our main focuses was on simulating the flow inside a combustion chamber, which is installed upstream of a rocket nozzle. As a first step to complete the simulation code suitable for the development of the combustion chamber, the gas phase combustion code is applied. Large Eddy Simulation (LES) code was developed in order to compute unsteady flows in turbomachinery. The code with cavitation model was applied to simulate unsteady phenomena related to cavitating flows in an inducer of a rocket engine turbopump. A simulation concerning flows around rotor blades in a fan was also performed, which is aimed at further improvement in the prediction accuracy of the developed code. Direct numerical simulation of a turbulent channel flow at $Re_\tau = 2320$ was performed in order to improve turbulence models to be applicable in high Reynolds number wall-turbulence. The visualized flow field and the turbulent statistics suggest that the fine-scale structures gather each other only in the low-speed large-scale structures. The energy transfer from larger-scale structures to smaller-scale ones is dominant.

**Keywords**: H-2A rocket, injector flow, rocket turbopump, cavitation, large eddy simulation, wall turbulence, direct numerical simulation

Understanding the physics of the internal flow of a rocket engine is essential for developing a highly reliable space launch vehicle. Until recently, the development of Japanese rockets was largely based on trial and error, i.e. an iterative cycle of trial design and experimental verification. Recent progress in computational fluid dynamics has changed this approach, as numerical simulation is now playing a major role in the development of rockets and rocket engines built today.

## 1. Injector simulation

This year, one of our main focuses was on simulating the flow inside a combustion chamber, which is installed upstream of a rocket nozzle[1]. Combustion chamber of a rocket engine is operated under very high temperature and pressure compared to the general industrial combustor. Therefore, there are many numerical difficulties treating the variety of the phenomena inside the combustion chamber of a rocket engine; for example, two phase flow (surface tension), breakup of the liquid phase, atomization, phase transition, real gas effect and combustion under high pressure should be reasonably and carefully considered. As a first step to complete the simulation code suitable for the development of the combustion chamber, the gas phase combustion code[2, 3] is applied; this code has been used for rocket nozzle flow and SRB gas leaking problems. The code incorporates the standard finite reaction rate model for the $H_2$-$O_2$ reaction. Figure 1 shows the static temperature for single co-axial injector configuration[4]. Although there still remains some intermittent behavior of the flow, the flame structure is captured by the simulation on the whole.

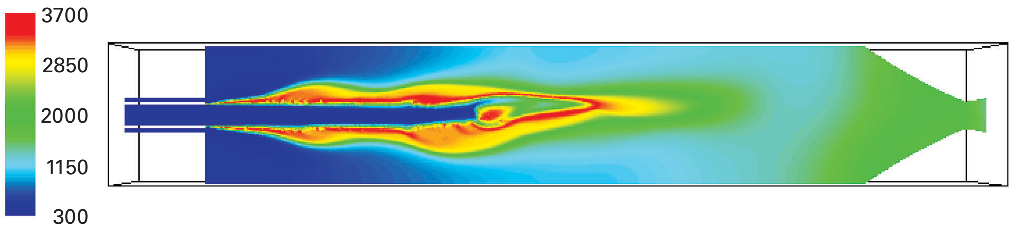


Fig. 1 Static temperature [K] for single co-axial injector configuration[4].

## 2. Turbomachinery simulation

To achieve operation at high rotational speed and low inlet pressure, rocket engine turbopumps are generally equipped with an axial-flow inducer stage. Under such operating conditions, cavitation develops on the suction side of the blades and near their tip. As the inlet pressure is decreased and local pressure becomes lower than the vapor pressure, cavitation gradually develops and finally leads to the breakdown of inducer performance. In addition, cavitation instabilities, such as rotating cavitation and cavitation surge, are often observed in experiments and cause serious shaft vibration and/or blade stress fluctuations. Therefore, it is an important issue to understand the physical mechanism of unsteady cavitation phenomena.

Computational Fluid Dynamics (CFD) is becoming an important tool for designing and developing reliable turbomachinery. For the study of static characteristic of cavitation, computations with Reynolds Averaged Navier-Stokes Simulation (RANS) are often carried out and some reliable results are obtained. However, we cannot predict cavitation-related unsteady phenomena with RANS since it is essentially based on the time-averaging concept and models dynamics of all turbulent eddies. On the other hand, a large eddy simulation (LES) directly deals with eddy dynamics resolved with the computational grids, and it is suitable for computing unsteady flows, such as cavitation. In the last fiscal year, we developed LES code for accurate computations of unsteady flows in turbomachinery, and then performed a computation of non-cavitating flows of a multistage centrifugal pump and did preliminary tests for cavitating flows. In this fiscal year, we have carried out two representative simulations; the first one is on cavitating flows in an inducer of a rocket engine turbopump to validate cavitation model in the code. The second one is a simulation regarding the internal flow of turbomachinery, which is aimed at further improvement in the prediction accuracy of the developed code.

Our LES code solves the Navier-Stokes equations of incompressible flow, in which dynamic Smagorinsky model is implemented as sub grid scale (SGS) model. The code is based on finite element method with hexahedral elements and has the second order accuracy in time and space[5]. By the multi-frame of reference function based on an overset method, it is possible to compute rotor-stator interactions[6]. For computation of cavitating flows, we have implemented the cavitation model proposed by Okita et al.[7] The evolution of cavitation is represented by the source/sink of vapor phase in incompressible liquid flows, and compressibility is taken into account through the low Mach number assumption.

The first topic is an analysis concerning the cavitating flows in an inducer. A test inducer in this study was originally designed for a rocket engine turbopump, which has three helical blades with swept-back leading edge. The total number of the finite elements for LES is about 8 million. The calculations performed at the designed operation point. Figure 2 shows instantaneous cavitation structures in the inducer for different cavitation number cases, $\sigma = 0.10$ and $\sigma = 0.05$. In $\sigma = 0.10$, cavity structures locally develop and are located along the tip leakage flow on each blade. As the cavitation number becomes small, the cavitation is generated in broader regions, especially on the blade surface and near the casing wall. It is found that the cavitation obtained in this result is symmetric, i.e., equal-length-like cavitation is detected, and the cavity rotates with the same rotational speed of the blades. Figure 3 indicates frequency spectra of pressure fluctuations on the casing (for cavitating flow case and non-cavitating flow case), which are sampled at six different axial locations. Several peaks appear in the spectra for both cases. The component with a large amplitude at a frequency of 150 [Hz] corresponds to the blade passing frequency (BPF) and its amplitude does not depend on whether the flow is cavitating or non-cavitating. In addition to the peaks at the BPF and its harmonics components, there exist large peaks at lower frequencies in the cavitating flow case and they must be related to the cavitation instability. To

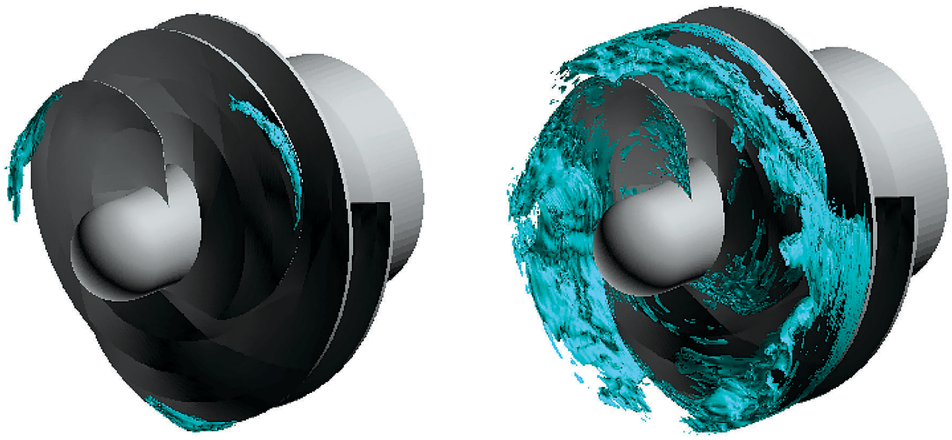

Fig. 2 Instantaneous cavity structures in an inducer for $\sigma = 0.10$ (left) and $\sigma = 0.05$ (right) (blue-colored surfaces represent iso-surface of void ratio 4%).

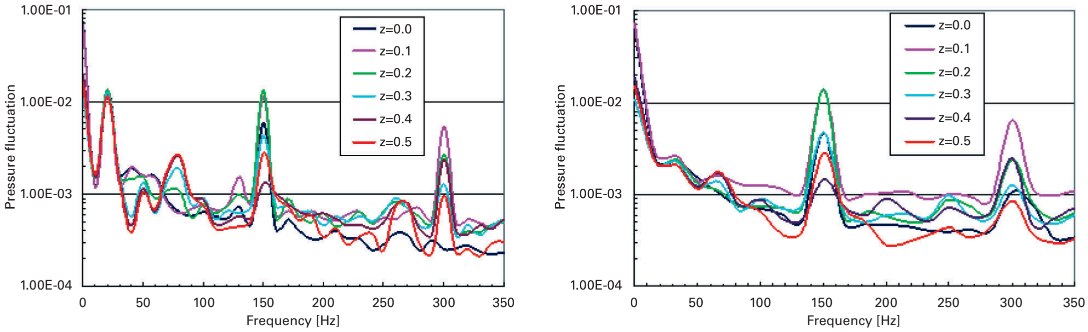


Fig. 3 Spectra of pressure fluctuations on the casing wall (left: cavitating flow with $\sigma = 0.05$, right: non-cavitating flow).

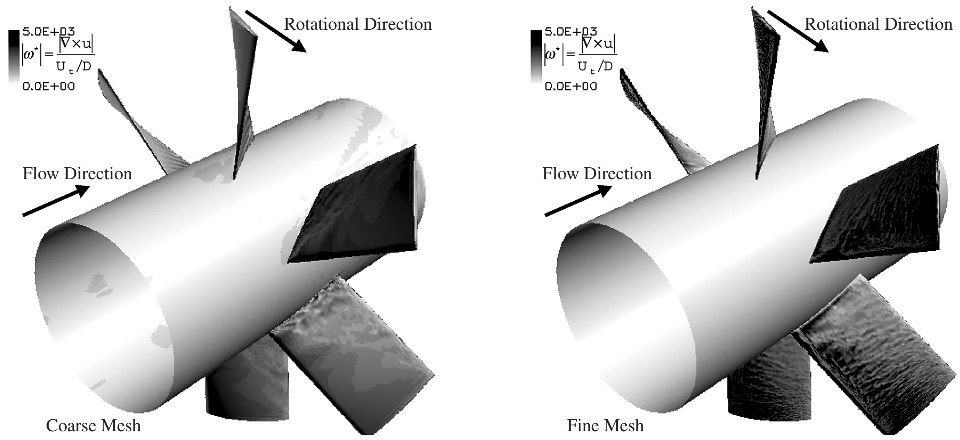


Fig. 4 Distributions of vorticity magnitude on hub and rotor blades surface (left: coarse mesh, right: fine mesh).

present a comprehensive scenario of unsteady phenomena of cavitation instability, long-time simulations will be needed in the future work.

The second topic is the result concerning flow around rotor blades in a fan[8]. A test fan in this study is an axial-fan with 6 rotor blades. Two kinds of computational meshes were applied in order to investigate effects of mesh resolution on computed flow field. The first mesh is a coarse one composed of about 3 million elements, and the second mesh is a fine one composed of about 30 million elements. The fine mesh resolves turbulent boundary layer (TBL) on the rotor blades, while the second mesh does not. Figure 4 shows a comparison of instantaneous distributions of vorticity magnitude. The results from the two cases essentially differ in that the later shows streak-like structures near the blade tip and large-scale structures near the hub while former shows only large-scale structures near the hub. Figure 5 shows instantaneous distributions of the vorticity magnitude around the leading edge (X/C = 0~0.2) near the tip (R/D = 0.48). Although not shown in this paper, the vorticity distribution obtained by the coarse-mesh LES does not change in time. On the other hand, the fine-mesh LES successfully captured unsteadiness in the vorticity near the leading edge, which is most likely to be associated with the boundary layer's separation, transition to turbulence and subsequent reattachment.

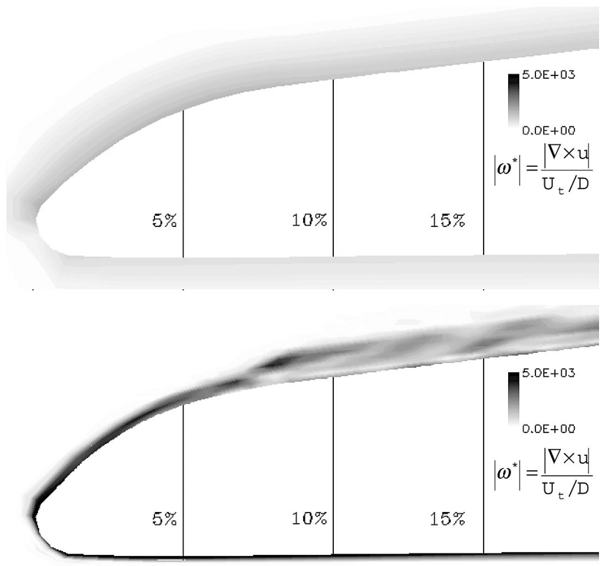


Fig. 5 Distributions of vorticity magnitude near leading edge of rotor blade at radius *R*/*D* = 0.48 (top: coarse mesh, bottom: fine mesh).

## 3. Channel flow simulation

Some fundamental characteristics of a turbulent channel flow at $Re_\tau = 2320$ are studied by means of direct numerical simulation (DNS). Our aim is to accumulate the essential knowledge on high-Reynolds number wall-turbulence, which can be used for improvement of turbulence models, such as subgrid-scale model in above-mentioned LES.

It is well known that near-wall streamwise vortices and streaky structures play a primary role in the transport mechanism on near-wall turbulence, at least, at low Reynolds number flows. On the other hand, the large-scale outer-layer structures and their relationship to the near-wall structures still remain unresolved. In the present study, DNS of turbulent channel flow at a Reynolds number of $Re_\tau = 2320$, which can be reached by the most powerful supercomputer system at this moment, is carried out to examine the relationship at high Reynolds numbers and the effect of the large-scale structures on the near-wall turbulence.

The numerical method used in the present study is a pseudo-spectral method. See Ref. [9] for the numerical procedures and parameters in detail. Hereafter, $u$, $v$, and $w$ denote the velocity components in the $x$-, $y$-, and $z$- directions, respectively. Superscript ($^+$) represents quantities non-dimensionalized with $u_\tau$ and $\nu$.

Figure 6 shows the ($y - z$) cross-stream plane of an instantaneous flow field, in which contours of the streamwise velocity fluctuation $u'$ are visualized. It is found that the large-scale structures exist from the center of the channel to the near-wall region. The spanwise scale at any $y$- location is roughly estimated at ~ $\delta$ based on the pre-multiplied energy spectra (not shown here). The streaky structures, of which spanwise spacing is about 100 $\nu / u_\tau$, exist only near the wall ($y^+ < 30$), while the large-scale structures exist from the central region of the channel to the region very near the wall ($y^+ \sim 30$).

In order to examine the relationship between the large-scale outer-layer structures and the near-wall structures, the instantaneous velocity field is decomposed into each structure with a resolution matched to its scale by means of a two-dimensional wavelet transform. Figure 7(a) shows the velocity field of the wavelet mode with the largest characteristic length. It is clearly observed that the mode corresponds to the large-scale structures of the instantaneous velocity field in Fig. 6. The velocity field corresponding to the fine-scale structures is shown in Fig. 7(b). It is found that these fine-scale structures gather each other only in the low-speed large-scale structures. Note that energy transfer between each mode can be calculated since all modes are defined mathematically. It is found that forward energy cascade from larger-scale structures to smaller-scale ones is dominant between these modes (not shown here).

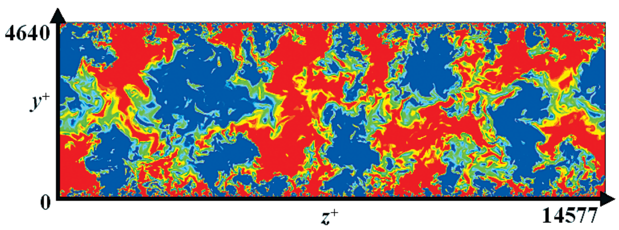


Fig. 6 Cross view of instantaneous velocity field. Contours of the streamwise velocity fluctuation, blue to red, $u'^+ = -1$ to $u'^+ = 1$. Total computational volume is 4640 and 14577 wall units in the $y$- and $z$-directions, respectively.

## Bibliographies

1) T. Shimizu, H. Miyajima and M. Kodera, "Numerical Study of Restricted Shock Separation in a Compressed Truncated Perfect Nozzle," AIAA Journal, Vol.44, No.3, pp.576–584, 2006.
2) Tohoku University Aerodynamic Simulation Code (TAS).
3) M. Kodera, T. Sunami, and K. Nakahashi, "Numerical Analysis of SCRAMJET Combusting Flows by Unstructured Hybrid Grid Method," AIAA 00–0886, Jan. 2000.
4) C. Schley, et al., "Comparison of Computational Codes for Modeling Hydrogen-Oxygen Injectors," AIAA 97–3302, Jul. 1997.
5) C. Kato, and M. Ikegawa, "Large Eddy Simulation of Unsteady Turbulent Wake of a Circular Cylinder Using the Finite Element Method," ASME-FED, 117, pp.49–56, 1991.
6) C. Kato, M. Kaiho, and A. Manabe, "An Overset Finite-Element Large-Eddy Simulation Method with Application to Turbomachinery and Aeroacoustics," Trans. ASME, 70, pp.32–43, 2003.
7) K. Okita, thesis of Osaka University (in Japanese), 2002.
8) Y. Yamade, at el "Large Eddy Simulation around Rotor Blades in an Axial-Flow Fan," (in Japanese) *Proceeding of 19th-CFD symposium*, 2005.
9) K. Iwamoto, N. Kasagi, and Y. Suzuki, "Direct numerical simulation of turbulent channel flow at $Re_\tau = 2320$," Proc. 6th Symp. Smart Control of Turbulence, pp.327–333, Tokyo, Japan, Mar. 2005.

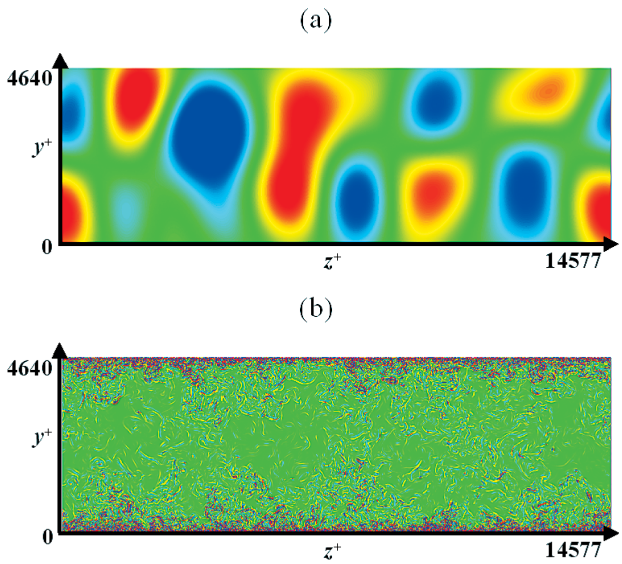


Fig. 7 Cross views of instantaneous velocity field for the wavelet modes. (a) Characteristic length $l^+ = 3600$ ($l / \delta = 1.6$); (b) $l^+ = 30$ ($l / \delta = 0.012$). Contours of the streamwise velocity fluctuation, blue to red, $u'^+ = -1$ to $u'^+ = 1$.

# ロケットエンジン内部流れのシミュレーション

プロジェクト責任者
藤井　孝藏　　宇宙航空研究開発機構 情報・計算工学センター

著者
清水　太郎　　宇宙航空研究開発機構 情報・計算工学センター
山西　伸宏　　宇宙航空研究開発機構 情報・計算工学センター
加藤　千幸　　東京大学生産技術研究所
笠木　伸英　　東京大学大学院工学系研究科
岩本　　薫　　東京理科大学理工学部機械工学科

国産ロケットの信頼性向上及び将来型宇宙輸送システムの開発に資するため、主要エンジン要素（燃焼器系・供給器系）で発生している諸問題を再現できるCFDコードを開発する。それらを概念設計・システム評価・不具合対策等に使用し、試作・試験のサイクルを短くすることを目標に、プロジェクトを進めた。本年度は、以下の3つのテーマについて解析を実施した。

これまでに解析を実施してきたロケットノズルの更に上流に存在する燃焼器内部流れを理解するため、解析を実施した。ロケット燃焼器は極めて高温・高圧のため、一般の産業機械に比べて数値解析上も多くの困難がある。例えば、2相状態、液相分裂、微粒化、相変化、実在気体効果、高圧下燃焼などを取り扱う必要がある。必要性とは裏腹に、現状、実問題に適用できる解析コードは皆無に等しい。そこで、本年度はこれまでにノズル横力の問題やSRBガスリークの問題解決で実績のあるコードを適用し、気相状態の燃焼によるベンチマークテストを実施し、おおむね良い結果が得られた。

ターボポンプ内の非定常な流れを精度良く解析するために、有限要素法に基づくLES (Large Eddy Simulation) 解析コードの開発を行った。解析コードにキャビテーションモデルを実装し、ロケットエンジンのインデューサ内部におけるキャビテーション流れに関する計算を行った。その結果、キャビテーションに起因すると思われる非定常現象を定量的に捉えることができた。さらに同コードの数値予測精度を高める目的で、軸流ファン動翼まわりの流れ解析を行った。格子解像度を上げた場合には翼面での縦渦構造の発達が見られ、乱流境界層の挙動の把握が可能であることを確認した。

高レイノルズ数壁乱流で用いることのできる高精度乱流粗視化モデルの構築を目的として、世界最大のレイノルズ数($Re_\tau = 2320$)平行平板間乱流直接数値シミュレーション（DNS）を行い、ウェーブレットを用いて乱流準秩序構造のダイナミクス解析を行った。大規模構造はアクティブに乱れを生成し、流れ場全体の乱れ生成機構の重要な役割を担っている。また微細構造は大規模構造の影響を受けて、大規模な低速領域に集まる（クラスター化）することを定性的かつ定量的に評価した。

キーワード：H-2A ロケット，インジェクター，ターボポンプ, LES，高レイノルズ数壁乱流, DNS